

Non-Fickian Diffusion in Thin Polymer Films

D. A. EDWARDS*

Courant Institute of Mathematical Sciences, New York University, New York, New York 10012

SYNOPSIS

Diffusion of penetrants through polymers often does not follow the standard Fickian model. Such anomalous behavior can cause difficulty when designing polymer networks for specific uses. One type of non-Fickian behavior that results is so-called case II diffusion, where Fickian-like fronts initially move like \sqrt{t} with a transition to a non-Fickian concentration profile and front speed for moderate time. A mathematical model is presented that replicates this behavior in thin polymer films, and an analysis is performed that yields relevant dimensionless groups for study. An unusual result is derived: In certain parameter ranges, the concentration profile can change concavity, reflecting Fickian behavior for short times and non-Fickian behavior for moderate times. Asymptotic and numerical results are then obtained to characterize the dependence of such relevant quantities as failure time, front speed, and mass transport on these dimensionless groups. This information can aid in the design of effective polymer protectant films. © 1996 John Wiley & Sons, Inc.

Keywords: non-Fickian diffusion • case II diffusion • polymer-penetrant systems • thin films

INTRODUCTION

Over the past several decades, much work, both experimental and theoretical, has been devoted to the study of polymer-penetrant systems. These new polymeric materials are fascinating for several reasons. From the practical side, they are extremely versatile and promise remarkable breakthroughs in a wide variety of fields. Polymer substrates have become widely used for microlithographic patterning, which has become an important industrial tool for VLSI chip etching.¹ Adhesives made from polymers are often much stronger than their conventional counterparts, which weigh more.^{2,3} Polymers are also being tested for on-site pharmaceutical administration.⁴⁻⁸ In addition, polymer films have shown great promise for providing barriers to toxins as protective clothing, equipment, or sealants.⁹⁻¹¹ It is this last application on which we focus in this paper.

From the theoretical side, the behavior such polymers exhibit continues to surprise. Experiments

constantly reveal new behavior in these systems; as such behavior is discovered, new and more detailed models for the physical processes are postulated. To verify these hypotheses, experimentalists are continually developing new measurement techniques to try to discern the exact physical processes involved.^{12,13}

Though all the physical mechanisms are not known, most scientists agree that one dominant factor is a viscoelastic stress in the polymer. This viscoelastic stress seems to be related to the concept of a *relaxation time*, which measures the time it takes one portion of the polymer entanglement network to react to changes in another portion. In certain polymer-penetrant systems, this stress, which is a nonlinear memory effect, is as important to the transport process as the well-understood Fickian dynamics.¹⁴⁻¹⁶ The type of polymers we wish to study are characterized by two states: *glassy* and *rubbery*. In the glassy region (denoted by sub- and superscripts *g*), the relaxation time is finite, so the stress is an important effect. In the rubbery region (denoted by sub- and superscripts *r*), the relaxation time is nearly instantaneous; hence, the memory effect is not as important there.^{11,16,17}

* To whom correspondence should be addressed at Department of Mathematics, University of Maryland, College Park, College Park, MD 20742-4015.

One type of non-Fickian behavior that results in such systems is so-called case II diffusion.¹⁷ In this phenomenon, described by Thomas and Windle,^{18,19} a Fickian-like front initially moves like \sqrt{t} . Then there is a transition period, occurring for moderate time, which cannot be described by Fickian dynamics. The concentration profile can be concave down, can move with constant speed, and can be quite sharp. Though other mathematical models for this type of diffusion have been formulated,²⁰ they did not incorporate the important effects of viscoelastic stress. We show in this paper that the system we are modeling is indeed a non-Fickian diffusion system. However, owing to the fact that we are dealing with thin films, the full second stage does not have time to develop. Such problems are common in experiments with and simulations of thin films; theoretically possible events do not occur due to the fact that the thinness of the film precludes the development of moderate- to long-time effects.²¹

In this paper, we formulate a model to explain this anomalous case II behavior. The model, which consists of a set of coupled partial-differential equations, will be simplified greatly once we consider the special case in which we are interested: cylindrically symmetric diffusion in thin annular films. It will quickly be shown that to leading order the problem reduces to one of studying a Cartesian thin film. The moving boundary-value problem that results can be solved using asymptotic, numerical, and singular perturbation techniques. We shall identify dimensionless groups that measure the relative effects of the different dynamical processes involved in the system in order to see which of them are dominant.

Insofar as we are modeling penetration of a substance through a thin polymer film, three important measurable quantities can be identified: the speed of the front separating the glassy and rubbery regions, the flux of the penetrant through the inner boundary of the film into the protected environment, and the time at which the polymer film can no longer serve as a useful protectant. In our analysis, each of these quantities is identified and related to the dimensionless parameters. Numerical computations and graphs will show the dependence of these very important quantities on our dimensionless groups. These computations should provide useful information to chemical engineers who wish to verify our model experimentally and, if our model is shown to be accurate, to those who wish to design safe and effective polymer films.

GOVERNING EQUATIONS

We begin with the following set of differential equations, which have been postulated as a mathematical model for non-Fickian diffusion in polymers²²⁻²⁵:

$$\dot{\tilde{C}}_i = \nabla \cdot [D(\tilde{C})\nabla\tilde{C} + E(\tilde{C})\nabla\tilde{\sigma}], \quad (1a)$$

$$\tilde{\sigma}_i + \beta(\tilde{C})\tilde{\sigma} = \eta\dot{\tilde{C}} + \nu\tilde{C}_i, \quad (1b)$$

where η and ν are constants. It is obvious that this model is derived from the standard diffusion equation, with an additional term in the flux. This additional term can be derived by assuming that the chemical potential depends not only on \tilde{C} but also on $\tilde{\sigma}$ ²⁵ given by

$$\tilde{\sigma} = \int_{-\infty}^i \exp\left\{-\int_{-\infty}^{i'} \beta(\tilde{C}(\tilde{x}, t'')) dt''\right\} [\eta\dot{\tilde{C}}(\tilde{x}, t') + \nu\tilde{C}_i(\tilde{x}, t')] dt'. \quad (1c)$$

This form for the chemical potential has been derived phenomenologically by observing the relevant processes that contribute to the qualitative features of case II diffusion, namely, molecular diffusion and viscoelastic stresses.

Note that by substituting eq. (1c) into eq. (1a), we may reduce our system to a single partial integrodifferential equation. Because $\tilde{\sigma}$ follows the evolution eq. (1b), which is quite reminiscent of the one for viscoelastic stress, we will refer to $\tilde{\sigma}$ as a "stress" throughout this paper. The right side of eq. (1b) shows that, in this paper, the stress will depend not only on the concentration but also on the time derivative of the concentration. Other forms for the dependence of $\tilde{\sigma}$ upon \tilde{C} and its derivatives are discussed by Cohen and White.²⁶

The model equations (1) are general enough that swelling of the polymer can be taken into consideration,²⁷ though we shall ignore swelling effects for the purposes of this paper. This is because the film will not swell enough to affect its thickness significantly, and it is the order of magnitude of the thickness that dictates the qualitative structure of the solution.

The term $\beta(\tilde{C})$ is worthy of special attention. Note from eq. (1c) that $\beta(\tilde{C})$ controls the strength of the "memory" of the polymer. Therefore, $\beta(\tilde{C})$ is the inverse of the relaxation time, and its dependence on \tilde{C} will be important and nonnegligible. However, experiments have shown that variations in the relaxation time *within* states seem to contribute little to the overall behavior. Therefore, we

average the relaxation time in each state and use the average as its value there. Thus we have

$$\beta(\tilde{C}) = \begin{cases} \beta_g, & 0 \leq \tilde{C} \leq \tilde{C}_* \\ \beta_r, & \tilde{C} > \tilde{C}_*, \end{cases} \quad (2)$$

where \tilde{C}_* is the value of \tilde{C} at which the glass-rubber transition takes place.

In addition, in the polymer-penetrant systems we wish to study, the diffusion coefficient often, though not always, increases dramatically as the polymer goes from the glassy to the rubbery state.²⁸ However, changes *within* states are less important. Hence, we perform the same averaging as we did with $\beta(\tilde{C})$ to obtain the following form for $D(\tilde{C})$:

$$D(\tilde{C}) = \begin{cases} D_g, & 0 \leq \tilde{C} \leq \tilde{C}_* \\ D_r, & \tilde{C} > \tilde{C}_*. \end{cases} \quad (3)$$

This form for $D(\tilde{C})$ mimics the formulation in Hui et al.²⁸ In order to simplify the problem, we assume that E is a constant. More discussion of various physically appropriate forms for $D(\tilde{C})$ and $E(\tilde{C})$ can be found in Cohen and White.²⁶

Because we know that the relaxation time in the glassy polymer is finite, whereas in the rubber it is instantaneous, we let $\beta_g/\beta_r = \epsilon$, where $0 < \epsilon \ll 1$ will become our perturbation parameter. We consider diffusion in an annular film that is cylindrically symmetric. Therefore, we need only consider variations in \tilde{r} , where $\tilde{r}_i \leq \tilde{r} \leq \tilde{r}_c$. Because we are trying to model a polymer film that could be used in protective clothing, we assume that the shell is very thin. Because the ratio of the relaxation times between glassy and rubbery is so large, ϵ is often on the order of 10^{-8} to 10^{-6} . Therefore, to model a 1-mm-thick film surrounding a moderately sized item to be protected, we should scale in the following manner:

$$\tilde{r}_i = (1 - b\epsilon^{1/2})\tilde{r}_c, \quad b = O(1),$$

because $\epsilon^{1/2} \approx 10^{-7/2}$ is an appropriate scaling for this physical situation.

Using these facts, we may then make the following substitutions:

$$x = \frac{1}{b\epsilon^{1/2}} \left(1 - \frac{\tilde{r}}{\tilde{r}_c} \right), \quad t = \tilde{t}\beta_g, \quad C(x, t) = \frac{\tilde{C}(\tilde{r}, \tilde{t})}{\tilde{C}_c},$$

$$\sigma(x, t) = \frac{\tilde{\sigma}(\tilde{r}, \tilde{t})}{\nu\tilde{C}_c}, \quad (4a)$$

$$C(x, t) = C^0(x, t) + o(1),$$

$$\sigma(x, t) = \sigma^0(x, t) + o(1). \quad (4b)$$

Note that we have used the relaxation time in the glassy polymer as our typical time scale. This is reasonable insofar as this time scale is of a physically observable order, namely, seconds or minutes.

Following experimental evidence, we see that the diffusion coefficient in the rubbery region is much greater than that in the glassy region.¹⁹ In fact, some authors have chosen to let $D_r = \infty$.²⁸ We obtain a similar result in a more rigorous way if we set $D_r = D_0\epsilon^{-1}$, because, if $\epsilon = 0$, we have $D_r = \infty$; however, in our perturbation analysis, as $\epsilon \rightarrow 0$, we have that D_r only becomes very large. Certainly this infinite limit could be reached in various ways; we choose $D_r = D_0\epsilon^{-1}$ because it yields a dominant balance in the equations that follow.

Since all of our parameters are piecewise constant, we may combine equations (1) into a single partial-differential equation. Substituting equations (4) into this result, we have the following, to leading order in the glassy region:

$$C_{tt}^{0g} = \kappa_g^2 \epsilon^{-1} C_{xxt}^{0g} - C_t^{0g} + \alpha_g^2 \epsilon^{-1} C_{xx}^{0g}, \quad s(t) < x < 1, \quad (5a)$$

where

$$\kappa_g^2 = \frac{D_g + \nu E}{\tilde{r}_c^2 \beta_g b^2}, \quad \alpha_g^2 = \frac{\beta_g D_g + \eta E}{\tilde{r}_c^2 \beta_g^2 b^2}.$$

In addition, eq. (1b) becomes

$$\sigma_t^g + \sigma^g = \gamma C^g + C_t^g, \quad (5b)$$

where $\gamma = \eta/\nu\beta_g$. In the rubbery region, we have

$$C_{tt}^{0r} = \kappa_r^2 \epsilon^{-2} C_{xxt}^{0r} - \epsilon^{-1} C_t^{0r} + \alpha_r^2 \epsilon^{-3} C_{xx}^{0r}, \quad 0 < x < s(t), \quad (6a)$$

where

$$\begin{aligned} \kappa_r^2 &= \chi_D + \epsilon \chi_\nu, & \chi_D &= \frac{D_0}{\tilde{r}_c^2 \beta_g b^2}, & \chi_\nu &= \frac{\nu E}{\tilde{r}_c^2 \beta_g b^2}, \\ \alpha_r^2 &= \chi_D + \frac{\epsilon^2 \eta E}{\tilde{r}_c^2 \beta_g^2 b^2}, \\ \sigma_l^r + \epsilon^{-1} \sigma^r &= \gamma C^r + C_l^r. \end{aligned} \tag{6b}$$

Equations (5a) and (6a) also hold for σ^g and σ^r , respectively. Note that to leading order curvature effects are unimportant, and we simply have the equations for a thin film in Cartesian coordinates.

Because we have assumed our parameters to be piecewise constant, we are now faced with a moving boundary-value problem. We must then consider conditions at our front $x = s(t)$. First, we require that at the moving front the concentration C must be at the specified transition value C_* :

$$C^{0g}(s(t), t) = C^{0r}(s(t), t) = C_*. \tag{7}$$

Note that this condition is different from the discontinuity in concentration at the moving front that one might expect to see in more standard systems.²⁹

In addition, we assume that the stress is continuous at the moving front³⁰:

$$\sigma^g(s(t), t) = \sigma^r(s(t), t). \tag{8}$$

Finally, we use a Stefan-like condition at the front, which implies that the flux used up in the change of state propels the front along. Then, our front condition becomes the following²²:

$$\begin{aligned} -\epsilon^{-1/2} [[D(C_*) + \nu E] C_x^0]_s + b \nu E (1 - \epsilon^{-1}) \\ \times \frac{\sigma(s(t), t)}{-b \epsilon^{1/2} \dot{s}} = -ab^2 \tilde{r}_c^2 \beta_g \epsilon^{1/2} \dot{s}, \end{aligned}$$

where a is a constant and we have used eq. (8). Here $[\cdot]_s = \cdot^g(s^+(t), t) - \cdot^r(s^-(t), t)$ and the dot above s represents differentiation with respect to t .

Here a is the *state-change* parameter. It relates the magnitude of the flux differential to the speed of the moving boundary. In a Stefan melting problem, this constant would be related to the specific heat of the melting substance. However, here the interpretation is more subtle and is discussed in more detail below. We note that, if the film is to have any practical value at all, a must be very large; that is, it takes a large difference in flux to move the front a small amount. Therefore, in order to yield a dominant balance in what follows, we let $a = a_0 \epsilon^{-2}$ and to leading order we have

$$-\dot{s} \chi_D C_x^{0r}(s(t), t) - \chi_\nu \sigma(s(t), t) = a_0 \dot{s}^2. \tag{9}$$

This type of moving boundary condition is non-standard and can lead to computational difficulties.²²

We now wish to consider the penetration of some substance into this film. We assume that initially the polymer is dry:

$$C^{0g}(x, 0) = 0. \tag{10a}$$

Using the nondimensional form of eq. (1c) for σ , we see that, if the polymer is initially dry, it must be unstressed:

$$\sigma^{0g}(x, 0) = 0. \tag{10b}$$

However, one could just as easily define other forms for the stress that would include thermodynamic or other mechanisms for “prestressing” to occur in a dry polymer. Because σ itself occurs in eq. (9), we see that such alternative boundary conditions would affect the evolution of the front.

On the outside of the film, we assume that there is an infinite supply of penetrant at the saturation value of the film:

$$C^{0r}(0, t) = 1. \tag{11}$$

This is an idealization of the surface boundary condition postulated by Long and Richman³¹ and Hui et al.³² If we wished, we could have let the concentration start at 0 and then quickly transition to 1 on a time scale such as t/ϵ . Note that this would be the time scale associated with the rubbery polymer. This would affect our results only in a narrow initial layer; the main results regarding front speed would remain the same. From equations (10a) and (11), we immediately deduce that $s(0) = 0$.

For the inside of the film, we apply a *radiation condition*, which indicates that the flux through the inside of the film is proportional to the difference between the concentration at the edge of the film and the concentration at the interior of the protected body, which we assume to be zero:

$$\begin{aligned} J(1, t) &= -[D(C)C_x^0(1, t) + \nu E \sigma_x^0(1, t)] \\ &= k \epsilon^{1/2} C^0(1, t), \end{aligned} \tag{12}$$

where k is a constant measuring the permeability of the inner surface. (In fully dimensional form, k would also include b and \tilde{r}_c .)

Next, we examine the question of failure of the film. First, we define a function $M(t)$, which is the

accumulated magnitude of the flux through the inner boundary:

$$\dot{M} = k\epsilon^{1/2}C^0(1, t), \quad M(0) = 0. \quad (13)$$

We note that $M(t)$ is a strictly increasing function of t . Then, we may define the failure time, t_f , to be t_m , which is the point at which $M(t_m) = M_{\max}$, where M_{\max} is the maximal tolerance of flux given by toxicity, spoilage, or other considerations. This is the *flux-limited case*. However, it is possible that, if the flux through the inner boundary is small, the front separating the two regions will reach the inner boundary at some *penetration time*, t_p , before t_m . If the rubbery state of the polymer film is useless for protectant purposes (as is shown below), then the failure time, t_f , should be defined as t_p . This is the *front-limited case*. Now, we have all the equations necessary to facilitate a further consideration of our problem.

PRELIMINARY AND BOUNDARY-LAYER RESULTS

We begin by solving the case where $k = k_0\epsilon^{-1/2}$. Then, for $t < t_p$ (that is, the time frame in which the polymer is in both the glassy and the rubbery states), equations (12) and (13) become

$$D_g C_x^{0g}(1, t) + \nu E \sigma_x^{0g}(1, t) = -k_0 C^{0g}(1, t), \quad (14)$$

$$\dot{M} = k_0 C^{0g}(1, t), \quad M(0) = 0. \quad (15)$$

$k_0 = 0$ corresponds to an impermeable inner surface; $k_0 \rightarrow \infty$ corresponds to a superpermeable inner surface. In this paper we examine the cases of impermeability and general permeability but not superpermeability. Now, letting $\epsilon \rightarrow 0$ in order to begin our perturbation solution, our equations become particularly simple. We begin by solving in the glassy region. Here we have that

$$0 = \kappa_g^2 C_{xxt}^{0g} + \alpha_g^2 C_{xx}^{0g}. \quad (16)$$

Unfortunately, because we have neglected the highest order time derivative, we cannot find a solution to eq. (16) that satisfies all our boundary conditions. Therefore, we must construct an initial layer.

We introduce the following variables:

$$\tau = \frac{t}{\epsilon}, \quad C^{0g}(x, t) \sim C^{0+}(x, \tau). \quad (17)$$

Making these substitutions into eq. (5a), we have the following, to leading order:

$$C_{\tau\tau}^{0+} = \kappa_g^2 C_{xx}^{0+}. \quad (18)$$

In addition, eq. (5b) becomes (to leading order)

$$\sigma_\tau^{0+} = C_\tau^{0+}.$$

Because σ and C have the same initial condition, we see that $\sigma^{0+} = C^{0+}$. Therefore, our boundary conditions (7), (10a), and (14) become

$$C^{0+}(0, \tau) = C_*, \quad C^{0+}(x, 0) = 0, \quad (19a)$$

$$(D_g + \nu E)C_x^{0+}(1, \tau) + k_0 C^{0+}(1, \tau) = 0. \quad (19b)$$

Integrating eq. (18) once with respect to τ , and using our facts about the initial conditions, we have

$$C_\tau^{0+} = \kappa_g^2 C_{xx}^{0+}. \quad (20)$$

We begin by trying to find a steady-state solution for this equation. Such a solution $C_s(x)$ is given by setting the left-hand side of eq. (20) equal to 0 and using equations (19). Then, we have

$$C_s(x) = C_* \left(1 - \frac{xk_g}{k_g + 1} \right), \quad (21)$$

where $k_g = k_0 / (D_g + \nu E)$. k_g measures the relative strength of the permeability with respect to the flux term in the glassy region. Note that with this definition of C_s , C^g always remains in the proper range.

Letting $w^+(x, \tau) = C_s(x) - C^{0+}(x, \tau)$, we have the operator in eq. (20) with the new boundary conditions

$$w^+(0, \tau) = 0, \quad w_x^+(1, \tau) + k_g w^+(1, \tau) = 0, \\ w^+(x, 0) = C_* \left(1 - \frac{xk_g}{k_g + 1} \right). \quad (22)$$

Equation (20) is simply the heat equation on a finite domain. Using the eigenfunction expansion

$$w^+(x, \tau) = \sum_{n=0}^{\infty} w_n^+(\tau) \sin \lambda_n x, \quad (23)$$

where $\lambda_n = -k_g \tan \lambda_n$, we have

$$w_n^+(\tau) = w_n^+(0) \exp(-\lambda_n^2 \kappa_g^2 \tau),$$

where

$$w_n^+(0) = \frac{C_*}{2\lambda_n}.$$

Now, we have that

$$C^{0+}(x, \tau) = C_* \left[1 - \frac{xk_g}{k_g + 1} - \sum_{n=0}^{\infty} \frac{1}{2\lambda_n} \exp(-\lambda_n^2 \kappa_g^2 \tau) \sin \lambda_n x \right]. \quad (24)$$

We note that, because eq. (5a) also holds for σ^g , eq. (24) is also our representation for σ^{0+} .

Thus, we see that, at the beginning of the experiment, the polymer quickly equilibrates to some new initial state commensurate with *whatever* boundary conditions are imposed at $x = 0$. This equilibration, though it takes place in the *glassy* polymer, occurs on a time scale that is on the order of the relaxation time in the *rubbery* polymer. This is due to the fact that it is the rubbery polymer that must coexist with the outer boundary.

Equation (21) now gives us the new initial conditions for our outer problem, namely, that $C^{0g}(x, 0) = C_s(x)$ and $\sigma^{0g}(x, 0) = C_s(x)$. Using these facts, we have

$$C^{0g}(x, t) = C_* [1 - f(t)(x - s)],$$

$$f(0) = \frac{k_g}{k_g + 1}. \quad (25)$$

We can use eq. (25) to simplify eq. (15), yielding

$$\dot{m} = k_g [1 - f(t)(1 - s)], \quad m(0) = 0,$$

$$m(t) = \frac{M(t)}{C_*(D_g + \nu E)}. \quad (26)$$

Here we have normalized by $C_*(D_g + \nu E)$, which is a measure of the effective diffusion coefficient in the rubbery polymer, insofar as this is how our graphs will be drawn.

Now, we examine the concentration field in the rubbery region. To leading order, eq. (6a) becomes

$$0 = \alpha_r^2 C_{xx}^{0r}, \quad (27)$$

so, using the applicable boundary conditions [equations (7) and (11)], our solution is

$$C^{0r} = 1 - \frac{(1 - C_*)x}{s}. \quad (28)$$

For $t > t_p$, our system is completely in the rubbery state, so it consists of eq. (27), eq. (11), and our new flux condition from eq. (12) replacing eq. (14):

$$C_x^{0r}(1, t) = 0. \quad (29)$$

The solution of this system is trivially $C^{0r} \equiv 1$. Therefore, we see that, as soon as the state-change boundary reaches the inner boundary of the polymer, the polymer immediately becomes saturated. This lends credence to our claim that t_p is an appropriate choice for our failure time if we have not yet reached t_m .

Note that, for $t = t_p$, we have that $s = 1$, so eq. (28) becomes

$$C^{0r} = 1 - (1 - C_*)x. \quad (30)$$

Therefore, there must be another boundary layer around $t = t_p$. This is once again obvious from the fact that we have neglected the highest order derivative with respect to time. Because the solution is discontinuous for all $x > 0$, we need stretch only time:

$$\bar{\tau} = \frac{t - t_p}{\epsilon^2}, \quad C^{0r}(x, t) \sim C^{0-}(x, \bar{\tau}).$$

We could also have stretched time by ϵ , but the equation that results has no solution that can match to a bounded solution as $\bar{\tau} \rightarrow -\infty$. Therefore, this equilibration takes place on a time scale that is even faster than the relaxation time of the rubbery region. To leading order, eq. (6a) becomes

$$C_{\bar{\tau}}^{0-} = \kappa_r^2 C_{xx}^{0-}, \quad -\infty < \bar{\tau} < \infty, \quad 0 \leq x \leq 1, \quad (31)$$

where we have used the fact that $C^{0-}(x, \infty) = 1$. In addition, we have

$$C^{0-}(0, \bar{\tau}) = 1, \quad (32a)$$

$$C^{0-}(x, -\infty) = 1 - (1 - C_*)x, \quad (32b)$$

$$C_x^{0-}(1, \bar{\tau}) = 0, \quad \bar{\tau} > 0. \quad (32c)$$

Note the extra condition on $\bar{\tau}$ in eq. (32c).

There is a slight ambiguity about what conditions to impose at $x = 1$ for $\bar{\tau} < 0$. Rewriting $s(t)$ in terms of our new variables, we see that, because $\dot{s}(t_p) \neq 0$, we have $s(t) \sim 1 + \epsilon^2 \dot{s}(t_p) \bar{\tau} + o(\epsilon^2)$, so to leading order we see that $s(\bar{\tau}) = 1$. Therefore, our expres-

sions for the front speed in the outer region for $t < t_p$ must hold in the inner region for $\bar{\tau} < 0$. Thus, we could use the concentration condition (7):

$$C^{0-}(1, \bar{\tau}) = C_*, \quad \bar{\tau} < 0. \quad (33a)$$

Alternatively, we could use the flux condition (9), which simply requires that the flux be continuous at $t = t_p$. Therefore, we have from eq. (30) that

$$C_x^{0-}(1, \bar{\tau}) = -(1 - C_*), \quad \bar{\tau} < 0. \quad (33b)$$

We will resolve that ambiguity while demonstrating the following amazing simplification: The solution is the same (within transcendently small corrections) if we restrict our operator (31) to the region $\bar{\tau} > 0$ and use an *initial* condition given by eq. (32b). This statement can be interpreted in three different ways, as follows.

1. Because the change of state is complete at $t = t_p$, the problem is fundamentally different, so it is not necessary to continue our boundary layer for $\bar{\tau} < 0$. Mercifully, eq. (6a) has a solution for $\bar{\tau} > 0$ that is as smooth as necessary, so there are no troubling discontinuities in the system.

2. If we use eq. (33a) as our boundary condition, we may introduce the quantity $w^-(x, \bar{\tau}) = 1 - (1 - C_*)x - C^{0-}(x, \bar{\tau})$, which yields the operator in eq. (31) with the following boundary conditions:

$$\begin{aligned} w^-(x, \infty) &= -(1 - C_*)x, & w^-(0, \bar{\tau}) &= 0, \\ w^-(x, -\infty) &= 0, & w_x^-(1, \bar{\tau}) &= 0, \quad \bar{\tau} > 0, \\ w^-(1, \bar{\tau}) &= 0, & \bar{\tau} < 0. \end{aligned} \quad (34)$$

However, we see that this system is quiescent for $\bar{\tau} < 0$, so we may as well begin at time $\bar{\tau} = 0$.

3. Similarly, if we use eq. (33b), eq. (34) becomes

$$w_x^-(1, \bar{\tau}) = 0, \quad \bar{\tau} < 0,$$

and once again we have a quiescent system for $\bar{\tau} < 0$.

Therefore, we are free to reduce our problem from a very complicated problem on a fully infinite interval to a much simpler one on a semiinfinite interval. Letting $w^-(x, \bar{\tau}) = 1 - C^{0-}(x, \bar{\tau})$, we have the operator in eq. (31) on the interval $\bar{\tau} > 0$ with the boundary conditions

$$w^-(0, \bar{\tau}) = 0, \quad w^-(x, 0) = (1 - C_*)x, \quad w_x^-(1, \bar{\tau}) = 0.$$

We now see that our boundary conditions are analogous to those in eq. (22). The only difference is that in this system $k_g = 0$, which implies that $\lambda_n = (n + \frac{1}{2})\pi$. Performing the same sort of analysis as before, we have that

$$\begin{aligned} C^{0-}(x, \bar{\tau}) &= 1 - \sum_{n=0}^{\infty} \frac{2(-1)^n(1 - C_*)}{(2n + 1)^2\pi^2} \\ &\exp\left[-\left(n + \frac{1}{2}\right)^2 \pi^2 \kappa_r^2 \bar{\tau}\right] \sin\left[\left(n + \frac{1}{2}\right)\pi x\right]. \end{aligned} \quad (35)$$

To complete our solution, we now consider the stress in the rubbery region. Equation (6b) becomes $\sigma^{0r} \equiv 0$ to leading order. This is consistent with our understanding that the change of state from glass to rubber reduces the stress in the polymer. It also means that there must be a boundary layer around $x = s(t)$ to match the discontinuous values of σ in each region. Introducing the boundary layer variables

$$\zeta = \frac{x - s(t)}{\epsilon}, \quad \sigma^{0r}(x, t) \sim \sigma^{0-}(\zeta, t) + o(1),$$

eq. (6b) becomes, to leading order,

$$-s\sigma_t^{0-} + \sigma^{0-} = 0,$$

$$\sigma^{0-}(0, t) = \sigma^{0g}(s(t), t), \quad \sigma^{0-}(-\infty, t) = 0,$$

where the right-hand side has vanished, because there is no boundary layer in C . Therefore, we have

$$\sigma^{0-}(\zeta, t) = \sigma^{0g}(s(t), t)e^{\zeta/s}. \quad (36)$$

Now, we have a full description of m , C , and σ given by equations (24) to (26), (28), (35), and (36). However, most of these descriptions are dependent on the front position, $s(t)$. Therefore, in order to complete the solution of our problem, we must track the front, which we begin in the next section.

FRONT EVOLUTION FOR SMALL TIME

In order to examine the evolution of the moving front $s(t)$, we use our results from the previous section. Using eq. (28) in eq. (9), we have

$$\frac{\chi_D(1 - C_*)}{s} - \frac{\chi_r \sigma(s(t), t)}{\dot{s}} = a_0 \dot{s}. \quad (37)$$

We note that we may use eq. (37) to obtain a short-time asymptotic solution for $s(t)$. By using the fact that $\sigma^{0g}(0, 0) = C_*$ and letting $s(t) \propto t^{1/2}$ (which yields a dominant balance), we have

$$s(t) \sim \sqrt{\frac{2t}{p_1}},$$

$$p_1 = \frac{a_0}{\chi_D(1 - C_*)} = \frac{a_0 \bar{r}_c^2 \beta_g b^2}{D_0(1 - C_*)}. \quad (38)$$

Thus, trivially we see that $a_0 > 0$, which is not true of all polymer-penetrant systems of this type.²⁵ Here, p_1 measures the ratio of the flux needed to move the front along (represented by the numerator) to the effective diffusion coefficient of the rubbery region (given by the denominator). We see, then, that by measuring the initial progression of our front, we can measure the parameter a , because all of the other parameters in eq. (38) would be given in a particular experiment.

Our expression for $s(t)$ in eq. (38) would hold whenever $t^{1/2}$ is large compared with other larger powers of t —that is, when $t \ll 1$. Therefore, we see that, for small t , the front speed does not depend on k . This matches our physical intuition; we would not expect the speed of the front near the *outer* boundary to be affected by the properties of the *inner* boundary. In addition, for small t , the front moves proportional to $t^{1/2}$, consistent with Fickian theory. The reason for this is that the nonlinear memory effects have not yet had time to develop.

Letting $u = p_1 s^2$ and rewriting eq. (37), we have

$$\dot{u} = 1 + \sqrt{1 - p_2 u \left[\frac{\sigma(s(t), t)}{C_*} \right]}, \quad u(0) = 0,$$

$$p_2 = \frac{4\chi\nu C_*}{\chi_D(1 - C_*)} = \frac{4\nu EC_*}{D_0(1 - C_*)}. \quad (39)$$

Therefore, we see that, if $\sigma(s(t), t)$ is relatively easy to calculate, we have a simple expression for $u(t)$ [and hence $s(t)$]. Here, p_2 measures the relative contributions to the flux from the stress term (numerator) and the concentration gradient term (denominator).

Equation (39) also yields several clues to the qualitative behavior of our solution. We immediately see that σ must remain bounded, a result we could have expected on physical grounds. Note from eq. (39) that our front u can never move at speeds faster than a constant. What we would expect to see, how-

ever, were we able to monitor the system for all time, is a transition from the small-time behavior $\dot{u} = 2$ to a long-time behavior where \dot{u} is some other constant. This is one observed characteristic of non-Fickian diffusion.²⁰ However, we note that the front will always reach the inner boundary in this formulation; hence, we would not expect to see the long-time behavior fully develop in experiments. This completes our analysis for small time. We next examine a special, simpler case before proceeding with the full-blown analysis.

FRONT EVOLUTION: THE NEAR-IMPERMEABLE CASE

We begin with the *near-impermeable* case, where $k = o(\epsilon^{-1/2})$, so $k_0 = 0$, which simplifies our equations. Equation (14) becomes

$$D_g C_x^{0g}(1, t) + \nu E \sigma_x^{0g}(1, t) = 0, \quad (40)$$

so we see that, to leading order, there is no flux through the inner film boundary; hence, t_m is a bad measure of failure. Thus, we are in the front-limited case, and we use t_p as our failure time.

With $k_0 = 0$, $\lambda_n = (n + \frac{1}{2})\pi$ in eq. (23), so eq. (24) becomes

$$C^{0+}(x, \tau) = C_* - \sum_{n=0}^{\infty} \frac{C_*}{(2n+1)\pi} \times \exp\left[-\left(n + \frac{1}{2}\right)^2 \pi^2 \kappa_g^2 \tau\right] \sin\left[\left(n + \frac{1}{2}\right)\pi x\right]. \quad (41)$$

We note that eq. (41) is also our representation for σ^{0+} .

Because $C^{0g}(x, 0) \equiv C_*$, we see that our front conditions are automatically satisfied for all t , so $f(t) \equiv 0$, and eq. (25) becomes

$$C^{0g}(x, t) \equiv C_*. \quad (42)$$

Then, substituting eq. (42) into eq. (5b) and using our boundary condition that $\sigma^{0g}(x, 0) = C^{0g}(x, 0) \equiv C_*$, we have

$$\sigma^{0g} = C_* e^{-t} + \gamma C_*(1 - e^{-t}). \quad (43)$$

We immediately see that σ^{0g} varies monotonically from C_* at time $t = 0$ to $C_*\gamma$ as $t \rightarrow \infty$. Therefore, σ^{0g} either increases or decreases as the experiment

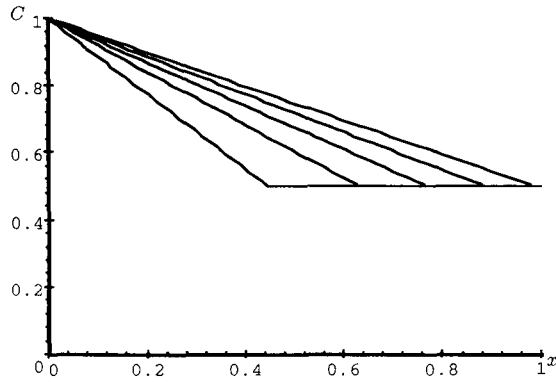


Figure 1. C vs. x for $p_1 = 1$; $p_2 = 0.3$; $\gamma = 0.8$; $C_* = \frac{1}{2}$; and $t = 0.1, 0.2, 0.3, 0.4,$ and 0.5 .

progresses, depending on the sign of $\gamma - 1$. Using eq. (43), we see that eq. (39) assumes a simple form:

$$\dot{u} = 1 + \sqrt{1 - p_2 u [e^{-t} + \gamma(1 - e^{-t})]},$$

$$u(0) = 0. \quad (44)$$

We also know that $u \leq p_1$, so we may deduce a requirement on our parameters that ensures that our discriminant is never negative:

$$p_1 p_2 < \min\{1, \gamma^{-1}\}. \quad (45)$$

We see, then, that the entire solution depends on the three dimensionless groups p_1 , p_2 , and γ .

Equation (44) is a simple first-order ordinary differential equation for $u(t)$. We solve eq. (44) using a standard fourth-order Runge-Kutta method to construct graphs of C^{0s} , C^{0r} , and s for various parameter ranges. In addition, we shall run many experiments and plot t_p vs. various parameters to see if we gain some sort of insight into the parameter dependence.

To obtain some qualitative feel for the behavior of our solution, we first solve some simple cases analytically. If either p_1 or $p_2 \rightarrow 0$, the leading-order solution of eq. (44) is

$$u = 2t, \quad t_p = \frac{p_1}{2}. \quad (46)$$

Note this is the solution given by eq. (38). In addition, we see that in this case there is no non-Fickian diffusion, because there is not enough time for the transition phase to develop. Note also that the penetration time depends linearly on p_1 , which varies as the square of the width of the film b . This is perfectly consistent with our statement that $s(t)$

varies as $t^{1/2}$. Next, we consider the case where $\gamma = 1$. Then, we have

$$\frac{2}{p_2} \left[1 - \sqrt{1 - p_2 u} + \log\left(\frac{1 + \sqrt{1 - p_2 u}}{2}\right) \right] = t, \quad (47)$$

$$t_p = \frac{2}{p_2} \left[1 - \sqrt{1 - p_1 p_2} + \log\left(\frac{1 + \sqrt{1 - p_1 p_2}}{2}\right) \right]. \quad (48)$$

Note that, in the limit that p_1 or $p_2 \rightarrow 0$, equations (47) and (48) reduce to eq. (46).

Figure 1 shows a graph of C vs. x for various parameters and various times. The graph illustrates the progression of the front, as well as the discontinuity in C_x that drives the motion of the front. Figure 2 shows a graph of σ vs. x for the same parameters and times. Note that, because $\gamma < 1$, the stress in the glassy polymer decreases with respect to time. Note also the relaxation effect, which dramatically decreases the stress in the polymer as it changes from glassy to rubbery. Here, $\epsilon = 0.002$, which makes for relatively sharp fronts. The fronts seen experimentally would only be steeper when one considers that ϵ is normally much smaller. Figure 3 is a graph of a typical profile of $s(t)$ vs. t . Note that the profile is nearly parabolic, as predicted by eq. (46).

Figure 4 shows a graph of $t_p - p_1/2$ vs. p_1 for various γ . As expected, because we have subtracted out the linear dependence of t_p on p_1 given by eq. (46), we have only terms of quadratic and higher order left. Note that this approximation holds even when p_1 is not small, with the error being no more

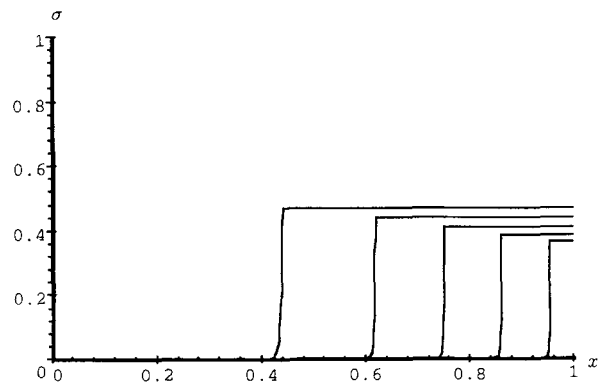


Figure 2. σ vs. x for $p_1 = 1$; $p_2 = 0.3$; $\gamma = 0.8$; $C_* = \frac{1}{2}$; $\epsilon = 0.002$; and $t = 0.1, 0.2, 0.3, 0.4,$ and 0.5 .

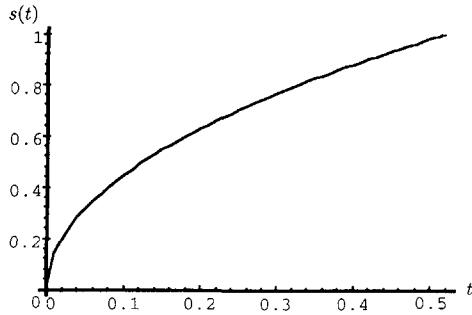


Figure 3. $s(t)$ vs. t for $p_1 = 1, p_2 = 0.3, \gamma = 0.8$.

than 10%. This is because, as p_1 gets larger, by eq. (45) we know that p_2 must become smaller, so eq. (46) still holds. As p_1 increases, so does t_p . The reason for this can be deduced from eq. (37). Rearranging, we have

$$\frac{1}{s} - \frac{p_2}{4C_*} \frac{\sigma(s(t), t)}{\dot{s}} = p_1 \dot{s}. \quad (49)$$

In this formulation, the flux remains relatively constant. Therefore, if p_1 decreases, \dot{s} must increase in the right-hand side of eq. (49), implying a smaller t_p .

Figure 5 shows a graph of t_p vs. p_2 for various p_1 . Note that, for small p_2 , $t_p \approx p_1/2$, as predicted by eq. (46). Here we see that, as p_2 decreases, the stress contribution in eq. (49) becomes negligible. Because the stress contribution is negative, this implies that, at any s , \dot{s} grows as p_2 decreases, implying a smaller t_p .

Figure 6 shows a graph of t_p vs. γ for various p_2 . Note that the entire graphed region is within 20% of the value $p_1 = 0.375$ predicted by eq. (46). As γ decreases, eq. (43) tells us that $\sigma(s(t), t)$ decreases. Therefore, by the reasoning described above, we see that t_p would also decrease.

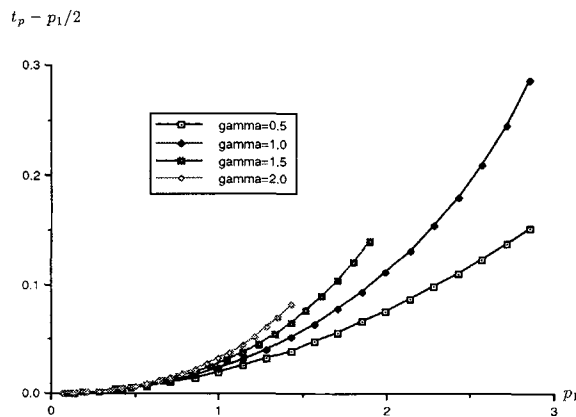


Figure 4. $t_p - p_1/2$ vs. p_1 for $p_2 = 0.333$ and various γ .

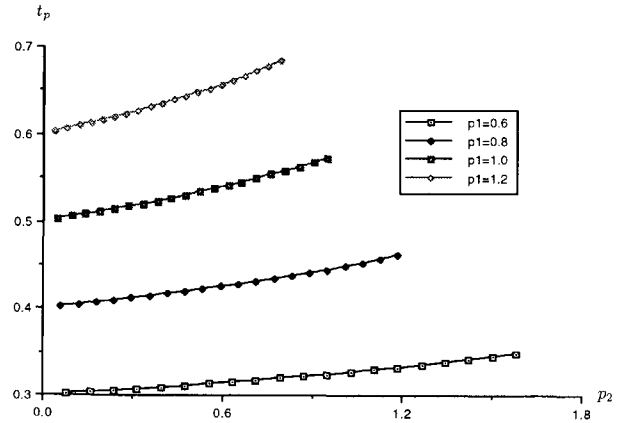


Figure 5. t_p vs. p_2 for $\gamma = 0.5$ and various p_1 .

FRONT EVOLUTION: GENERAL PERMEABILITY

We have gained some insight into our problem by solving the simpler case of an impermeable inner boundary; we will now solve the case of general permeability. Our first step is to solve for the stress in the glassy region. Making the substitution $\sigma^{0g}(x, t) = \sigma^a(x, t) + C^{0g}(x, t)$, we have

$$\sigma_t^a + \sigma^a = (\gamma - 1)C^{0g}, \quad \sigma^a(x, 0) = 0, \quad (50)$$

which yields

$$\sigma^{0g}(x, t) = C_* \left\{ \gamma - (x - s)f - (\gamma - 1) \times \left[e^{-t} + \int_0^t e^{-(t-t')} f(t') [x - s(t')] dt' \right] \right\}. \quad (51)$$

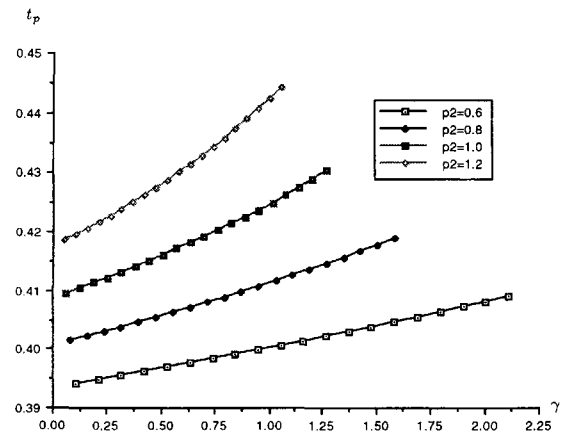


Figure 6. t_p vs. γ for $p_1 = 0.75$ and various p_2 .

Now we use equations (25) and (51) in eq. (14):

$$(D_g + \nu E)f + \nu E(\gamma - 1) \left[\int_0^t e^{-(t-t')} f(t') dt' \right] = k_0[1 - (1 - s)f]. \quad (52)$$

For small time, solving eq. (52) directly for f is expedient. Therefore, we have

$$f(t) = \frac{1}{1 + k_g(1 - s)} \times \left\{ k_g - \frac{\gamma - 1}{p_3 + 1} \left[\int_0^t e^{-(t-t')} f(t') dt' \right] \right\}, \quad (53)$$

where $p_3 = D_g/\nu E$. p_3 measures the relative contributions to the flux in the glassy region from the concentration and stress gradients.

To get our flux front condition, we can substitute eq. (51) evaluated at $x = s(t)$ into eq. (49):

$$\frac{\dot{s}}{s} - \frac{p_2}{4} \left\{ \gamma - (\gamma - 1) \left[e^{-t} + \int_0^t e^{-(t-t')} \times f(t') [s(t) - s(t')] dt' \right] \right\} = p_1 \dot{s}^2. \quad (54)$$

Alternatively, we can substitute directly into eq. (39):

$$\dot{u} = 1 + \sqrt{1 - p_2 u \left\{ \gamma - (\gamma - 1) \times \left[e^{-t} + \int_0^t e^{-(t-t')} f(t') [s(t) - s(t')] dt' \right] \right\}}, \quad u(0) = 0. \quad (55)$$

Once again, we see that, if $p_2 \rightarrow 0$, the stress is not important, and eq. (38) becomes our solution for $s(t)$ for all time. Equations (53) and (55) now form a system of integrodifferential equations, which can be solved with a Runge-Kutta algorithm adapted to keep track of the integral terms. Since our flux at the inner boundary is no longer negligible, we must also solve eq. (26) to see if the failure time, t_f , is given by t_m or t_p .

By direct analogy with eq. (45), we see that we have solutions whenever

$$\frac{1}{p_1 p_2} > \max_t \frac{\sigma(s(t), t)}{C_*}.$$

We note from eq. (51) that, in the case $\gamma > 1$, the maximum of $\sigma(s(t), t)$ is trivially given by γC_* . However, in the case $\gamma < 1$, we must establish a maximum on the integral, which involves finding the maximum of $f(t)$. We begin by deriving a differential equation for $f(t)$ from eq. (53):

$$\dot{f} = -f + \frac{k_g(1 + \dot{s}f) - (\gamma - 1)f/(p_3 + 1)}{k_g(1 - s) + 1}. \quad (56)$$

We expect f always to be positive from eq. (25). To find the maximum, we solve eq. (56) for when the derivative is 0:

$$f = \frac{k_g}{k_g(1 - s) + 1 - k_g \dot{s} + (\gamma - 1)/(p_3 + 1)}. \quad (57)$$

Next, we note that, because $\sigma^0 > 0$, we see from eq. (49) that we have

$$\dot{s} < \frac{1}{p_1 s}.$$

Using that fact in eq. (57), we have

$$f < \frac{k_g p_1 s}{k_g p_1 s(1 - s) + p_1 s - k_g + (\gamma - 1)p_1 s/(p_3 + 1)}. \quad (58)$$

Now, considering the right-hand side of eq. (58) to be a function of s only, we see that we have a maximum when $s = 1/\sqrt{p_1}$. If $p_1 > 1$, this case occurs, in which case we have

$$f < \frac{k_g \sqrt{p_1}}{k_g \sqrt{p_1} + \sqrt{p_1} - 2k_g + (\gamma - 1)\sqrt{p_1}/(p_3 + 1)}.$$

However, if $p_1 < 1$, then we have

$$f < \frac{k_g p_1}{p_1 - k_g + (\gamma - 1)p_1/(p_3 + 1)}.$$

We denote the maximal values of f by f^* .

Therefore, using the fact that the maximal value of the bracketed quantity in the integrand is 1, we have that the integral must be bounded below $f^*(1 - e^{-t})$. Then, we see that

$$\max_t \frac{\sigma(s(t), t)}{C_*} = \max[\gamma, 1, \gamma - f^*(\gamma - 1)],$$

so

$$\frac{1}{p_1 p_2} > \begin{cases} \gamma, & \text{if } \gamma > 1, \\ 1, & \text{if } \gamma < 1 \text{ and } f^* < 1, \\ \gamma + f^*(1 - \gamma), & \text{if } \gamma < 1 \text{ and } f^* > 1. \end{cases} \quad (59)$$

In the limit that $k_0 \rightarrow 0$, recall that $f^* \rightarrow 0$, so eq. (59) reduces to eq. (45).

Unfortunately, owing to the integrals in equations (53) and (55), a Runge-Kutta algorithm for these equations requires that values of s and f must be stored for all time steps. This quickly becomes untenable if one uses small time steps. Therefore, it is expedient to transform equations (53) and (54) into purely differential equations.

Equation (56) is the transformation of eq. (53). Note that, in the case where $k_0 = 0$, we have $\dot{f} = -f$, $f(0) = 0$, which has zero for a solution, as was expected from our work in the previous section. From eq. (56) we can obtain an asymptotic solution for $f(t)$ for small time. Substituting equations (25) and (38) in eq. (56) and asymptotically expanding, we have

$$f \sim \left(\frac{k_g}{k_g + 1} \right) \left(1 + \frac{k_g}{k_g + 1} \sqrt{\frac{2t}{p_1}} \right). \quad (60)$$

Next we transform our solution of eq. (54). Using equations (52) and (56), we have

$$\ddot{s} = \left[\frac{1}{s} - 2p_1 \dot{s} \right]^{-1} \left\{ \frac{\dot{s}}{s} \left(\frac{\dot{s}}{s} - 1 \right) + p_1 s^2 - \frac{p_2}{4} \right. \\ \left. \times [\dot{s}(p_3 + 1) \{ k_g - [k_g(1 - s) + 1] f \} - \gamma] \right\}. \quad (61)$$

However, we note that, because $s(t) \propto t^{1/2}$ for small t , the right-hand sides of equations (56) and (61) become unbounded for $t \rightarrow 0$. Therefore, the solution process adopted is a combined approach: For small time, equations (53) and (55) are solved, because they are numerically stable for $t \rightarrow 0$. Then, at some intermediate time when memory storage becomes a problem, equations (56) and (61) are solved until either t_m or t_p is reached.

Finally, we perform asymptotic analyses on our remaining parameters. The case where $k_g \rightarrow 0$ has

already been addressed. When $k_g \rightarrow \infty$, eq. (56) becomes, to leading order,

$$\dot{f} = -f + \frac{1 + \dot{s}f}{1 - s}, \quad f(0) = 1,$$

the solution of which is

$$f(t) = \frac{1}{1 - s(t)}. \quad (62)$$

Because eq. (55) is analogous to eq. (44), we see that our results for p_1 small and $\gamma = 1$ still hold. Also, when $\gamma = 1$ or $p_3 \rightarrow \infty$, eq. (53) becomes

$$f(t) = \frac{k_g}{1 + k_g(1 - s)}. \quad (63)$$

We also see from eq. (26) that, if k_g is small but nonzero,

$$m(t) \sim k_g t, \quad t_m = \frac{M_{\max}}{C_* k_0}. \quad (64)$$

The work necessary to calculate the stress profile in this case is more difficult. First, we know that eq. (36) still holds in the rubbery region. In addition, owing to the form of eq. (5b), a linear profile in x for C implies a linear profile in x for σ . Therefore, it is sufficient to know the stress in two points. We choose the points $x = s(t)$ and $x = 1$. As long as we are using eq. (55) to track the progression of the front, which we do for the vast majority of the time involved, then $\sigma^{0g}(s(t), t)$ is available as a byproduct of this calculation. For the point $x = 1$, we may substitute eq. (25) evaluated at $x = 1$ into eq. (50) to obtain $\sigma^a(1, t)$. Then, $\sigma^{0g}(1, t)$ is easily calculated by adding this result to eq. (25) evaluated at $x = 1$. Once we have the values at these two points, we simply use the point-slope formula:

$$\sigma^{0g}(x, t) = \frac{\sigma^{0g}(s(t), t) - \sigma^{0g}(1, t)}{s - 1} (x - 1) + \sigma^{0g}(1, t).$$

Figure 7 shows C vs. x for various parameters and times. Note in this case that we have *two* linear profiles with a discontinuity in slope at $s(t)$. Also note that there is a change in concavity as the front progresses; for small times, the front is concave upward, as is standard in Fickian polymer-penetrant systems.³³ As was indicated above, this short-time behavior indicates that the effects of stress are not yet important. However, as time progresses, the graph

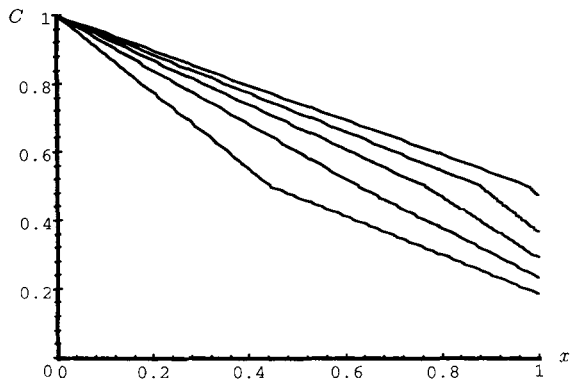


Figure 7. C vs. x for $p_1 = 1$; $p_2 = 0.3$; $p_3 = 0.5$; $k_g = 3$; $\gamma = 0.8$; $C_* = \frac{1}{2}$; $m_{\max} = \infty$; and $t = 0.1, 0.2, 0.3, 0.4,$ and 0.5 .

becomes concave downward, as seen in other simulations of non-Fickian systems.^{24,25} Thus, memory effects are starting to play a significant role. What is unique is the fact that the growing strength of this effect causes a concavity change. In other simulations, the concavity remains the same.²³⁻²⁵

Figure 8 shows σ vs. x for the same parameters and times. Note that in this case we have a slow increase in stress as we progress from the inner boundary outward. This corresponds to the stress slowly building as the concentration increases in the glassy region. We did not see such a profile in the impermeable case; there was no variation in C with respect to x . Once we reach the rubber-glass transition, there is a quick dropoff as the stress is released in the change of state. Though the trend is not as pronounced as in Figure 2, the maximal value of the stress is decreasing as time progresses, consistent with our choice of $\gamma < 1$.

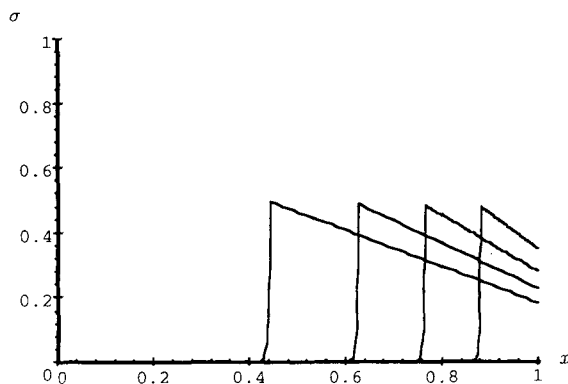


Figure 8. σ vs. x for $p_1 = 1$; $p_2 = 0.3$; $p_3 = 0.5$; $k_g = 3$; $\gamma = 0.8$; $C_* = \frac{1}{2}$; $\epsilon = 0.002$; $m_{\max} = \infty$; and $t = 0.1, 0.2, 0.3,$ and 0.4 .

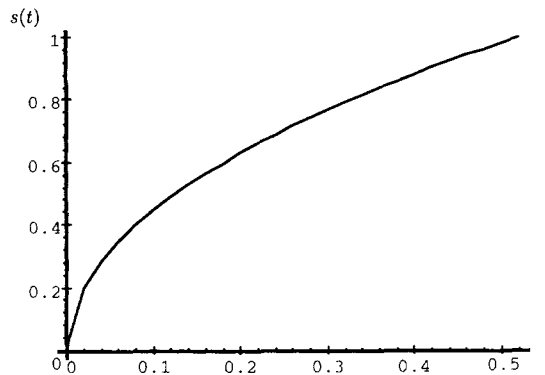


Figure 9. $s(t)$ vs. t for $p_1 = 1, p_2 = 0.3, p_3 = 0.5, k_g = 3,$ $\gamma = 0.8,$ and $m_{\max} = \infty$.

Figure 9 shows $s(t)$ vs. t for the same parameters. Note that there is very little change in the graph from the analogous Figure 3. Figure 10 shows the accumulated flux at the inner boundary $m(t)$ vs. t for the same parameters.

Figure 11 shows t_f vs. k_g for various values of m_{\max} . Note here that, because m_{\max} changes, in some cases the failure time is given by t_m and in others it is given by t_p . Note that, if it is given by t_m (that is, we are in the flux-limited case), the time decreases with increasing k_g . This is perfectly consistent with our interpretation of k_g as a measure of the permeability of the inner boundary. Compare the rather strong dependence of t_m on k_g with the rather weak dependence of t_p on k_g . This is due to the fact that k_g plays a secondary role in the evolution of the front position, coupled only through the integral term.

Figure 12 echoes the findings in Figure 11, showing a graph of t_f vs. p_3 for various k_g . We once again see the extreme dependence of t_f on k_g when we are in the flux-limited case. Note that, in all cases, the dependence of t_f on p_3 is negligible. Once again, this is due

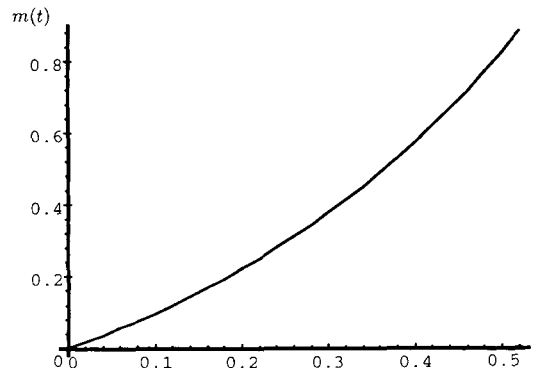


Figure 10. $m(t)$ vs. t for $p_1 = 1, p_2 = 0.3, p_3 = 0.5, k_g = 3, \gamma = 0.8,$ and $m_{\max} = \infty$.

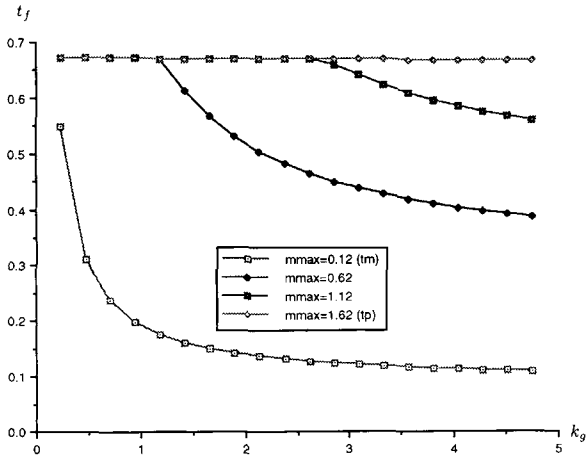


Figure 11. t_f vs. k_g for $p_1 = 1.2, p_2 = 0.5, p_3 = 1, \gamma = 1.5$, and various m_{max} .

to the fact that p_3 plays only a secondary role in the evolution of f , which itself plays only a secondary role in the evolution of s . This weak dependence is also evident in Figure 13. Note that, for all listed values of p_3 , the dependence of $t_p - p_1/2$ on p_3 is the same to the resolution of the graph. Note again that our expression $t_p \approx p_1/2$ is valid to within 10%.

Figure 14 shows t_p vs. k_g for various values of γ . Note the small scale of the t_p axis. As was indicated above, t_p varies very weakly with k_g . The important thing to note is the fact that, for $\gamma < 1$, t_p increases for increasing k_g , and, for $\gamma > 1$, t_p decreases for increasing k_g .

These results indicate the same general trends as we found in the impermeable case. However, the added layer of sophistication due to the introduction of permeability considerations yielded several important differences. There was the addition of two more parameters, k_g and p_3 , as dimensionless groups

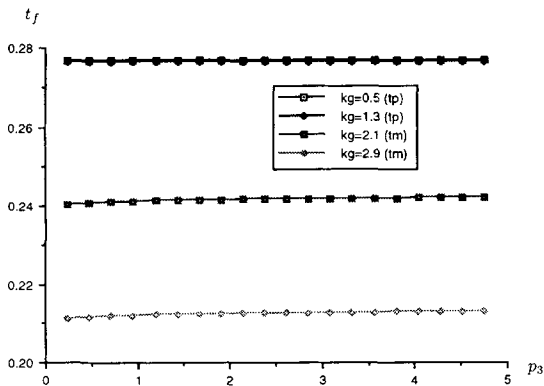


Figure 12. t_f vs. p_3 for $p_1 = 0.5, p_2 = 1.2, \gamma = 1.5, m_{max} = 0.31$, and various k_g .

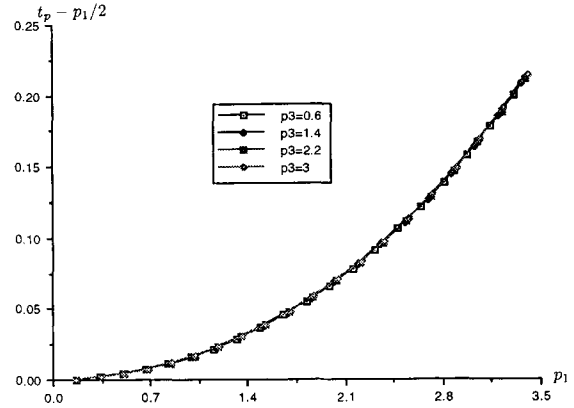


Figure 13. $t_p - p_1/2$ vs. p_1 for $p_2 = 0.25, k_g = 1, \gamma = 0.75, m_{max} = \infty$, and various p_3 .

worth examining. In addition, now the failure time, t_f , could be given by either t_m or t_p , which was not true in the impermeable case. Finally, the concentration profiles changed concavity, indicating the growing influence of the viscoelastic stress on the qualitative structure of the solution.

CONCLUSIONS

Protectant films made from polymers exhibit great potential for use under a wide variety of conditions. However, to custom-design polymer films efficiently for many different uses, a fuller understanding of the relevant physical processes must be gained. In this paper, we have presented a model for such films in the presence of a penetrant. By simplifying our complicated model while retaining features of the salient physical processes, we were able to obtain results that gave explicit dependence of our solutions

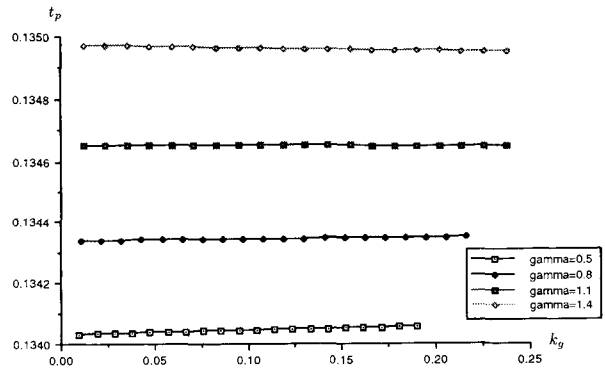


Figure 14. t_p vs. k_g for $p_1 = 0.25, p_2 = 2, p_3 = 0.5, m_{max} = \infty$, and various γ .

on various dimensionless groups of physical parameters.

When first exposed to a penetrant, the polymer equilibrates on a fast time scale—the relaxation time scale of the rubbery polymer, because the glassy polymer must change to rubbery near the outer boundary. This pseudoequilibrium provides a “true” initial condition for the rest of the dynamics. Then, over a much slower time scale, a moving state-change front progresses through the polymer. The time scale here is that of the relaxation time of the glassy polymer, because the dynamics of the glassy polymer determine the progression of the moving front. For small time, this front behaves in a Fickian manner, moving proportional to $t^{1/2}$ as given by eq. (38). The equation governing the movement of the front is capable of exhibiting the anomalous behavior of case II diffusion. However, with the time limitations imposed by such a thin film, such behavior cannot fully develop. Once the front has progressed all the way to the inner boundary of the film, the polymer, now totally in the rubbery state, equilibrates again by becoming totally saturated on a fast time scale.

There are two ways to characterize the failure of a polymer protectant film. First, if the front reaches the inner boundary and the film becomes saturated nearly immediately, then one would expect that the film would no longer have any protective value. However, if before that point the amount of flux through the inner boundary exceeds some tolerance threshold, then that time should be used as the time of failure. In this paper, we examined both possibilities.

First, we considered the case where the inner boundary was impermeable. In this case, our measurement of the failure time was totally dictated by the front movement. Our equations simplified, and we were able to reduce our system to a first-order nonlinear ordinary differential equation. By using a standard Runge-Kutta algorithm, we were able to obtain the dependence of the solution on various dimensionless groups. The failure time increased as p_1 increased, because as p_1 increases more flux is required to push the front along. The failure time also increased as p_2 or γ increased; this corresponds to a larger stress term, and the stress term retards front motion.

Next, we considered the case where the inner boundary had arbitrary, though moderate, permeability. The equations in this case were more complicated integrodifferential equations, and a more sophisticated numerical algorithm had to be used. The results in this section were similar to those in

the previous section, although there were several significant differences.

First, we found two new dimensionless groups upon which the solution depended. An interesting phenomenon developed in the concentration profiles: They changed concavity, something not seen in previous simulations of these equations. For small time, the graphs were concave upward, as is typical in standard Fickian systems.³³ This is consistent with the interpretation that for small time the effects of the stress, which are related to the memory, are not fully developed. However, as time progressed, the effects of memory became important, and the profile more closely resembled the profiles of non-Fickian polymer-penetrant systems.^{24,25} The stress built up slowly in the glassy region and then was quickly released during the change of state to the rubbery region, which is also consistent with non-Fickian behavior.^{23,24}

Also, in this case we now had to consider failure times caused not only by front penetration but also by flux considerations. The penetration time weakly increased as k_g and p_3 increased, because an increase in k_g or p_3 is weakly coupled to a larger stress term. In contrast, t_m decreased quite considerably with increasing k_g , because, the higher k_g is, the more penetrant can flow through the inner boundary.

The results of this paper lay the groundwork for further study of thin polymer films. We have introduced a mathematical model that is simple enough to analyze yet complicated enough to contain the salient nonlinear features. By doing so, we hope to have postulated a model that can be experimentally verified. If it is found to be valid, then its simplicity and the explicit parameter dependence in its solutions might aid chemical engineers in the design of safe and effective thin polymer films.

This work was performed under National Science Foundation grant DMS-9407531. Additional partial support was provided by the Center for Nonlinear Studies at Los Alamos National Laboratory, Air Force Office of Scientific Research grant F49620-94-I-0044, and National Science Foundation grant DMS-9501511. We thank Donald S. Cohen and Christopher Durning for their contributions, both direct and indirect, to this paper. Many of the calculations herein were performed using Maple.

NOMENCLATURE

Variables and Parameters

Units are listed in terms of length (L), mass (M), moles (N), or time (T). If the same letter appears

both with and without tildes, the letter with a tilde has dimensions, whereas the letter without a tilde is dimensionless. The equation where a quantity first appears is listed, if appropriate.

a	coefficient in flux-front speed relationship
b	measurement of width of film (4a)
$\tilde{C}(\cdot, \tilde{t})$	concentration of penetrant at position \cdot and time \tilde{t} ; units N/L^3 (1a)
$D(\tilde{C})$	binary diffusion coefficient for system; units L^2/T (1a)
$E(\tilde{C})$	coefficient preceding the stress term in the modified diffusion equation; units NT/M (1a)
$f(t)$	arbitrary function in expression for C^{0g} (25)
$J(x, t)$	flux at position x and time t ; units L^2/T (12)
k	coefficient in inner-surface boundary condition; units L^2/T (12)
$m(t)$	dimensionless version of $M(t)$, value $M(t)/C_*(D_g + \nu E)$ (26)
$M(t)$	accumulated flux through the inner boundary; units L^2/T (13)
n	indexing variable (23)
p	dimensionless parameter, variously defined by subscript (38)
\tilde{r}	distance coordinate in the curvilinear coordinate system; units L
$s(t)$	position of state-change front in the x -coordinate system (7)
\tilde{t}	time from imposition of external concentration; units T (1a)
$u(t)$	transformed front position; value $u = p_1 s^2$ (39)
$w(\cdot)$	dummy function used to simplify boundary-layer equations (22)
x	dimensionless distance coordinate in the thin-film coordinate system (4a)
α	dimensionless parameter, variously defined by subscript
$\beta(\tilde{C})$	inverse of the relaxation time; units T^{-1} (1b)
γ	dimensionless parameter; value $\eta/\nu\beta_g$ (5b)
ϵ	perturbation expansion parameter; value β_g/β_r (4a)
ζ	dimensionless spatial boundary layer variable
η	coefficient of concentration in stress evolution equation (1b); units ML^2/NT^3
κ	dimensionless parameter, variously defined by subscript
ν	coefficient of \tilde{C}_i in stress evolution equation (1b); units ML^2/NT^2

$\tilde{\sigma}(\cdot, \tilde{t})$	stress in polymer at position \cdot and time \tilde{t} ; units M/LT^2 (1a)
τ	dimensionless temporal boundary-layer variable
χ	dimensionless parameter, variously defined by subscript

Other Notation

c	as a subscript, used to indicate the characteristic value of a quantity (4a)
f	as a subscript, used to indicate the failure time
g	as a sub- or superscript, used to indicate the glassy state (2)
i	as a subscript, used to indicate the inner boundary
m	as a subscript, used to indicate the time at which the flux through the inner boundary exceeds some critical threshold
max	as a subscript, used to indicate the maximal value of M or m allowed before failure of the film
p	as a subscript, used to indicate the penetration time
r	as a sub- or superscript, used to indicate the rubbery state (2)
s	as a subscript, used to indicate the steady state of the initial layer equations (21)
*	as a subscript, used to indicate at the transition value between the glassy and rubbery states (2)
+	as a superscript on a dependent variable, used to indicate a boundary-layer expansion in the glassy region (17)
—	as a superscript on a dependent variable, used to indicate a boundary-layer expansion in the rubbery region
'	used to indicate a dummy variable of integration
—	used to indicate the internal layer near $t = t_p$
.	used to indicate differentiation with respect to t
$[\cdot]_s$	jump across the front $s(t)$, defined as $\cdot^g(s^+(t), t) - \cdot^r(s^-(t), t)$

REFERENCES AND NOTES

1. L. F. Thompson, C. G. Wilson, and M. J. Bowden, *Introduction to Microlithography*, ACS Symposium Series **219**, ACS, Washington, 1983.
2. E. Martuscelli and C. Marchetta (eds.), *New Polymeric Materials: Reactive Processing and Physical Properties*,

- Proceedings of International Seminar, Naples, June, 1987.
3. S. R. Shimabukuro, Ph.D. Thesis, California Institute of Technology, 1991.
 4. D. R. Paul and F. W. Harris (eds.), *Controlled Release Polymeric Formulations*, ACS Symposium Series **33**, ACS, Washington, 1976.
 5. T. J. Roseman and S. Z. Mansdorf (eds.), *Controlled Release Delivery Systems*, Marcel Dekker, New York, 1983.
 6. R. Langer, *Science*, **249**, 1527 (1990).
 7. P. J. Tarche, *Polymers for Controlled Drug Deliveries*, CRC Press, New York, 1991.
 8. J. Travis, *Science*, **259**, 289 (1993).
 9. J. S. Vrentas, C. M. Jorzelski, and J. L. Duda, *AIChE J.*, **21**, 894 (1975).
 10. C. A. Finch (ed.), *Chemistry and Technology of Water-Soluble Polymers*, Plenum, New York, 1983, Chap. 17.
 11. W. R. Vieth, *Diffusion In and Through Polymers: Principles and Applications*, Oxford, New York, 1991.
 12. R. C. Lasky, E. J. Kramer, and C. Y. Hui, *Polymer*, **29**, 1131 (1988).
 13. C. J. Durning, M. M. Hassan, H. M. Tong, and K. W. Lee, *Macromolecules*, **28**, 4234 (1995).
 14. W. R. Vieth and K. J. Sladek, *J. Colloid Sci.*, **20**, 1014 (1965).
 15. D. R. Paul and W. J. Koros, *J. Polym. Sci.*, **14**, 675 (1976).
 16. H. L. Frisch, *Polymer Eng. Sci.*, **20**, 2 (1980).
 17. J. Crank, *The Mathematics of Diffusion*, 2nd ed., Oxford, New York, 1976, Chap. 11.
 18. N. Thomas and A. H. Windle, *Polymer*, **19**, 255 (1978).
 19. N. Thomas and A. H. Windle, *Polymer*, **23**, 529 (1982).
 20. G. Astarita and G. C. Sarti, *Polym. Eng. Sci.*, **18**, 388 (1978).
 21. T. Z. Fu and C. J. Durning, *AIChE J.*, **39**, 1030 (1993).
 22. D. A. Edwards and D. S. Cohen, *SIAM J. Appl. Math.*, **55**, 662 (1995).
 23. D. A. Edwards, *SIAM J. Appl. Math.*, **55**, 1039 (1995).
 24. D. A. Edwards and D. S. Cohen, *IMA J. Appl. Math.*, **55**, 49 (1995).
 25. D. A. Edwards and D. S. Cohen, *AIChE J.*, **41**, 2345 (1995).
 26. D. S. Cohen and A. B. White, Jr., *SIAM J. Appl. Math.*, **51**, 472 (1991).
 27. R. A. Cairncross and C. J. Durning, *AIChE J.* (to appear).
 28. C. Y. Hui, K. C. Wu, R. C. Lasky, and E. J. Kramer, *J. Appl. Phys.*, **61**, 5137 (1987).
 29. J. Crank, *Free and Moving Boundary Problems*, Oxford, New York, 1984.
 30. W. G. Knauss and V. H. Kenner, *J. Appl. Phys.*, **51**, 5131 (1980).
 31. F. A. Long and D. Richman, *J. Am. Chem. Soc.*, **82**, 513 (1960).
 32. C. Y. Hui, K. C. Wu, R. C. Lasky, and E. J. Kramer, *J. Appl. Phys.*, **61**, 5129 (1987).
 33. D. A. Edwards, Ph.D. Thesis, California Institute of Technology, 1994.

Received July 14, 1995

Revised November 13, 1995

Accepted November 17, 1995